Published in final edited form as:
Eur J Pharmacol. 2011 October 15; 668(3): 435–442. doi:10.1016/j.ejphar.2011.02.045.

A CXCL8 receptor antagonist based on the structure of N-Acetyl-Proline-Glycine-Proline

Patricia L. Jackson[a], **Brett D. Noerager**[b], **Michael J. Jablonsky**[c], **Matthew T. Hardison**[a], **Bryan D. Cox**[c], **James C. Patterson**[c], **Boopathy Dhanapal**[d], **J. Edwin Blalock**[a], and **Donald D. Muccio**[c]

[a] Department of Medicine, Division of Pulmonary, Allergy and Critical Care Medicine and UAB Lung Health Center, University of Alabama at Birmingham, Birmingham, AL [b] Department of Biology, Chemistry, and Mathematics, University of Montevallo, Montevallo, AL [c] Department of Chemistry, University of Alabama at Birmingham, Birmingham, AL [d] Lipal Biochemicals AG Gundetswil, Switzerland

Abstract

A role for the collagen-derived tripeptide, N-acetyl proline-glycine-proline (NAc-PGP), in neutrophil recruitment in chronic airway inflammatory diseases, including COPD and cystic fibrosis, has recently been delineated. Due to structural similarity to an important motif for interleukin-8 (CXCL8) binding to its receptor, NAc-PGP binds to CXCR1/2 receptors, leading to neutrophil activation and chemotaxis. In an effort to develop novel CXCL8 antagonists, we describe the synthesis of four chiral isomers of NAc-PGP (NAc-L-Pro-Gly-L-Pro (LL-NAc-PGP), NAc-L-Pro-Gly-D-Pro (LD-NAc-PGP), NAc-D-Pro-Gly-L-Pro (DL-NAc-PGP), NAc-D-Pro-Gly-D-Pro (DD-NAc-PGP)), characterize them by circular dichroism and NMR spectroscopy, compare their structures to the equivalent region of CXCL8, and test them as potential antagonists of LL-NAc-PGP and CXCL8.

We find that LL-NAc-PGP superimposes onto the CXCR1/2 contacting $E^{29}S^{30}G^{31}P^{32}$ region of CXCL8 (0.59A rmsd for heavy atoms). In contrast, DD-NAc-PGP has an opposing orientation of key functional groups as compared to the $G^{31}P^{32}$ region of CXCL8. As a consequence, DD-NAc-PGP binds CXCR1/2, as demonstrated by competition with radiolabeled CXCL8 binding in a radioreceptor assay, yet acts as a receptor antagonist as evidenced by inhibition of CXCL8 and LL- NAc-PGP mediated neutrophil chemotaxis. The ability of DD-NAc-PGP to prevent the activation of CXC receptors indicates that DD-NAc-PGP may serve as a lead compound for the development of CXCR1/2 inhibitors. In addition, this study further proves that using a different technical approach, namely preincubation of NAc-PGP instead of simultaneous addition of NAc-PGP with radiolabeled CXCL8, the direct binding of NAc-PGP to the CXCL8 receptor is evident.

Address correspondence to: Patricia Jackson PhD (Address: 1918 University Blvd MCLM 898 Birmingham, AL 35294); phone number (205-934-3032); fax number (205-934-1446), plj@uab.edu.

Conflict of interest

The authors declare no conflicts of interest.

Index Words

inflammation; d-peptides; CXCL8; NAc-PGP; CXCR1; CXCR2

1. Introduction

The novel peptide N-acetyl-Pro-Gly-Pro (NAc-PGP) was initially described in an alkali eye injury model as a vigorous activator of and specific chemoattractant for neutrophils (Pfister et al., 1998; Pfister et al., 1995). The solution structure of this peptide was previously determined and was shown to be an extended structure in both water and DMSO (Lee et al., 2001). It exists as a mixture of the four possible *cis/trans* isomers of the two proline residues. We initially suspected NAc-PGP was capable of binding to CXCR1 and 2 as a result of noting its structural similarity to a receptor binding SGP motif of several ELR+ CXC chemokines, including CXCL8 (Weathington et al., 2006). We subsequently demonstrated that NAc-PGP caused *in vivo* and *in vitro* neutrophil chemotaxis and activation via action on CXCR 1 and 2 and further demonstrated that NAc-PGP competed with radiolabeled CXCL8 for binding to CXCR1/2 in a radioreceptor assay. This later observation has recently been questioned and one goal of the present study was to determine why there was no reproducibility found of our earlier findings. We found that this was likely due to a technical design flaw in the radioreceptor assay described by de Kruijf and coworkers (de Kruijf et al., 2010).

We have since measured significant amounts of NAc-PGP in human samples from patients with inflammatory diseases such as chronic obstructive pulmonary disease (COPD) and cystic fibrosis (O'Reilly et al., 2009a; Rowe et al., 2008; Weathington et al., 2006). We have identified an enzymatic cascade that can lead to the production of NAc-PGP from the extracellular matrix (Gaggar et al., 2008; O'Reilly et al., 2009b). Recently, we have also shown that a nonacetylated PGP peptide may be a distinguishing biomarker between acute and chronic lung transplant rejection (Hardison et al., 2009). The presence of NAc-PGP in human samples from diseases of interest, the lack of satisfactory therapeutics, and the possible new role of NAc-PGP as a biomarker underscores the need for better understanding of the peptide-receptor interactions.

The chirality, D- or L-, of an amino acid is determined by the relationship of the side chain group relative to the α-carbon, and has biological consequences. D-peptides are typically stable to enzymatic activity, i.e., proteases. D-peptides have been shown to have effects on neutrophils, for example, both the all D- and all L-isomers of the hexapeptide RRWWCR inhibit CXCL8 binding to and activation of human blood neutrophils (Hirayama et al., 2006). It is not known if the SGP motif of CXCL8 which binds to CXCR1 and CXCR2 receptors has a preferred chirality. All of these factors led us to further explore the peptide-chemokine receptor interactions of NAc-PGP. To this end, we have synthesized the four possible NAc-PGP isomers (LL-, LD-, DL-, DD-), analyzed their structures by circular dichroism and NMR, compared these structures to CXCL8, and measured their bioactivity. Using these data we hope to gain insight into the structural requirements for the chemoattractivity and peptide binding pocket structure, with the goal of obtaining CXCL8 antagonists with greater biologically activity and stability.

2. Materials and Methods

2.1 Cell Culture

Human neutrophils were isolated by density centrifugation using Histopaque. HL-60 cells were purchased from American Type Culture Collection and maintained under

recommended conditions. They were differentiated into CXCR1/2 positive neutrophil-like cells by incubations with 1.3% DMSO for 96 hours (Jacob et al., 2002).

2.2 Chemotaxis Assays

Indicated reagents were placed in the bottom wells of a 3-μm 96-well polycarbonate filter plate (Millipore) in 150 μl DMEM and 2 × 105 cells in 100 μl DMEM were added with 5% BSA to the top portion. The plates were incubated for 1.5h at 37°C in 5% CO_2. Micrographs of migrated cells on the bottom plate were made with an Olympus IX70 microscope and Perkin Elmer Ultraview equipment, and migration was standardized from cell counts such that chemotactic index = cells per high-powered field (experimental)/cells per high-powered field (media control), as previously described (Weathington et al., 2006).

2.3 Peptide Synthesis and Characterization

The four possible L- and D- isomers of NAc-PGP, (NAc-L-Pro-Gly-L-Pro, NAc-L-Pro-Gly-D-Pro, NAc-D-Pro-Gly-L-Pro, NAc-D-Pro-Gly-D-Pro) were synthesized as previously described (Lee et al., 2001). Isotopic and chemical purity were confirmed by NMR and circular dichroism (CD) spectroscopy. The peptide concentration was determined from the ^1H NMR spectrum of a solution of 60 μl 2.00 mM tryptophan (as determined by UV), 30 μl peptide, and 180μl D_2O, and measuring the ratio of the tryptophan aromatics to the peptide methyl, H^{β}, and H^{γ} peaks.

2.4 Radioreceptor Assay

5×10^5 neutrophils were placed directly in siliconized microfuge tubes. For controls, either buffer (RPMI 1640 w/25mM HEPES and 1% BSA) alone or unlabeled CXCL8 was added in a volume of 100 μl for a final concentration of 79.6 ng/ml. For experimental groups, DD-NAc-PGP was added in a volume of 100 μl for final concentrations of 0.75 mg/ml, 0.23 mg/ml, and 0.075 mg/ml. Cells were either placed at 4°C for 30 min before [125I]-CXCL8 (Perkin- Elmer, Waltham MA) or [125I]-CXCL8 was added simultaneously in 100 μl for a final concentration of 7.96 ng/ml. Cells were returned to 4°C for 90 min. Cells were washed three times in 1 ml buffer and counts/min (cpm) was determined using a Packard gamma radiation counter. Non-specific binding was determined using 10 fold excess of unlabeled CXCL8.

2.5 Circular Dichroism Spectroscopy

Circular Dichroism (CD) spectra were obtained on an AVIV model 62DS spectropolarimeter (Lakewood, NJ). Data were collected at 20°C at 2.0 mg/ml peptide in a 0.1 mm mountable cell. CD scans were run from 260 nm to 190 nm in 1.0 nm steps with 32 second averaging per point. Data were baseline corrected from an identical run of the appropriate blank, and smoothed with a 3rd order polynomial (window +/− 10 pts.). Ellipticity was reported in mdeg. For chiral isomer comparison, the slight differences in sample concentration were taken into account by multiplying spectra by an appropriate scaling factor.

2.6 NMR Spectroscopy

All samples were prepared at 40 mg/ml in 5 mm Shigemi microtubes at 250 μl, 90:10 H_2O:D_2O, at pH 5.5. Data were collected on Bruker DRX400 spectrometer at 293 K and referenced to internal DSS. 1D ^1H and ^{13}C, and 2D NOESY, TOCSY, HMQC-TOCSY, HMQC, and HMBC experiments were standard Bruker programs. 1D ^1H spectra were collected with water presaturation and a 5 sec. recycle time; 1D ^{13}C data were recorded with 16k scans. All 2D data were recorded with water suppression as 2k × 512 matrices. The HMBC was recorded in magnitude mode at 8 ppm ^1H and 180 ppm ^{13}C. All other 2D data

were recorded in phase-sensitive mode with TPPI at 8 ppm ^{1}H and 60 ppm ^{13}C. The NOESY data were acquired with a 1 sec mixing time, and the TOCSY and HMQC-TOCSY data with a 60 ms MLEV17 spin-lock pulse preceded by a 1ms trim pulse. The 2D data were processed with 300 shifted sinebells, zero-filled to 2k × 2k matrix, Fourier transformed, and baseline corrected.

2.7 Molecular Modeling

The NAc-PGP isomers were energy minimized with Sybyl 7.0 (Tripos, Inc.) without nOe constraints as discussed in Lee et al., 2001. The resulting NAc-PGP structures were matched with respect to the 11 backbone atoms or the 18 heavy atoms of CXCL8 $H^{29}S^{30}G^{31}P^{32}$(1ilq.pdb).

2.8 Molecular Dynamics (MD)

The molecular dynamics simulations were run using NAMD (Phillips et al., 2005). The input files and analysis were treated using the Visual Molecular Dynamics package (VMD) (Humphrey et al., 1996). The initial all trans NAc-PGP structures were created using the Sybyl package (SYBYL 7.3) in the extended conformation. The acetyl group was treated with the CHARM 22/27 ACP patch on the N-terminal (Mackerell, 2004). The peptides were encased in explicit TIP3 water molecules 12 Å in all directions. The dimensions of the periodic water box were 35 × 35 × 30 Å. The charge of the system was neutralized using sodium ions. Before the simulations, the system was treated to 10,000 steps of conjugate gradient minimization. The simulations were run at constant pressure (1 atm) and temperature (300K) for 2 ns in 2 fs steps. The structure of the entire system was recorded every 10 ps for later analysis. The long-range electrostatic interactions were treated using Particle Mesh Ewald (Cerutti et al., 2009). The short-range electrostatics and Van der Waals interactions had a distance cut-off of 12 Å. The simulations were run with and without the CMAP correction multiple times. It was found that the CMAP over-corrected for this system. When CMAP was used, the glycine ϕ and Ψ angles were conformationally restricted to 180° and 90°, respectively, with no interchange. The data presented was not simulated with the CMAP correction.

The analysis required a measurement that reflected the relative orientations of the N-terminal acetyl group in relation to the C-terminal carboxylic acid. An improper dihedral was defined between the C(Acetyl)-N(Pro_1)-C_α(Pro_3)-COO(Pro_3) which measures the orientations. The simulations yielded 200 frames, and each frame produced one measurement of the improper dihedral angle. The measurements of the improper dihedral angle were sorted into a histogram in 20° bins. Each histogram was fit to the Gaussian distribution.

3. Results

3.1 CD Analysis

CD spectra of proteins and peptides reflect both the secondary structure and the absolute chirality of the species in solution. The solution structures of the enantiomeric NAc-PGP isomer pairs, LL- and DD-, and LD- and DL-, are expected to be mirror images as seen (Fig. 1). This confirms the enantiomeric purity of the isomers. The LL- isomer spectrum has a large negative band at 200nm and stays negative at 185 nm. No band is present at 222 nm. This spectrum is consistent with a mainly random coil structure with possibly a small fraction of beta-strand. The lack of a positive band at 195 nm and a negative band at 222 nm precludes the existence of turn and helical components (Grathwohl and Wuthrich, 1976; Jacob et al., 2002). As expected, the magnitude and shape of the CD spectra are equal and opposite for the DD-isomer. The LD- and DL-isomer CD spectra are more complex, but are

still mirror images with equal magnitudes and shapes. The CD spectra analyses are further complicated because CD spectra are a weighted average of the four possible *cis/trans* isomer populations. Consequently, we used NMR spectroscopy to determine these *cis/trans* ratios, and to analyze the solution structures.

3.2 NMR Analysis

Determining exact structural differences of small peptides, especially of D- and L- isomers mixtures with *cis/trans* isomers, is difficult by CD, but is tractable by NMR. In general, the NMR spectra of an all D- or all L- isomer of the same peptide should be identical, whereas mixed chiral isomers should not. The 1H spectra for the LL- and DD-, and DL- and LD-isomers are essentially identical (Fig. 2), confirming the similar solution structures. The minor spectral differences can be attributed to slight resolution differences. The *cis* and *trans* isomers were distinguished by nOe contacts from the preceding residue to the proline H^{δ} or the H^{α}, and allowed for the complete ^{1}H and ^{13}C chemical shift assignments of all isomers (Lee et al., 2001). The carbon spectra of the enantiomers show identical chemical shifts for the LL- and DD-, and DL- and LD- isomers, and overall the four isomers are similar (Fig 3). In addition to the structural similarity of the mirror images, the *cis/trans* isomer ratios of the LL- and DD-, and of the DL- and LD- isomers are expected to be equal. The *cis/trans* isomer ratios should be tractable from both the ^{1}H and ^{13}C spectra, but because of overlap in the ^{1}H spectra, these were determined from the intensities of the glycine carbonyl, the Me carbonyl, and the methyl ^{13}C resonances (Table I). The *cis/trans* ratios among the four isomers were similar, with the *trans* isomer of a given proline always being dominant. However, when comparing the *trans/cis* ratios of Pro^{1} and Pro^{3}, Pro^{3} always had a lower *trans/cis* ratio. For example, the L-L-isomer had ratios of *trans-trans*--PGP to *trans-cis*-PGP of 59:41, and *trans-trans*--PGP to *cis-trans*--PGP of 70:30. For the same *trans/cis* ratios, the DL- and LD-isomers gave 63:37 and 72:28, a slightly higher amount of trans isomer (Table II). Finally, the 2D TOCSY and NOESY spectra of the LL- and DD-isomers were identical (as were the DL- and DL-isomers), and were similar to the DL- and LD-isomers. These data indicate no differences in either coupling constants or ^{1}H-^{1}H distances. The NOESY spectra showed no evidence of turns or helices as only i, i +1 nOe's were observed.

3.3 Molecular Modeling

The NMR and CD data are consistent with solution structures of NAc-PGP which are present in both *cis* and *trans* forms and which are in extended conformations. Energy minimization of each NAc-PGP chiral isomer gave families which had similar extended backbone structures, but with different orientations of the carbonyl oxygens and sidechains. The backbone atoms of the LL- and DD-isomers match well, but not all of the carbonyls and sidechains align. The ring and Me group of Pro-1 orient in opposite directions, as does the carbonyl. The carbonyls Pro-1 and Gly-2 differ by 45° and 90°, respectively. When viewed down the peptide backbone, these differences are evident, and are consistent with the orientations suggested by the Newman projections (Fig. 4). We aligned the minimized LL-NAc-PGP and DD-NAc-PGP structures to the $S^{30}G^{31}P^{32}$ of the previously published CXCL8 crystal structure (Fig. 5). For the LL- isomer, the 11 backbone atoms align almost identically to the CXCL8 backbone (0.45 A rmsd). The spatial arrangement of the carbonyls and sidechains are also almost identical to those in CXCL8 (0.59 A rmsd for all 18 heavy atoms). The DD- isomer backbone also matches well with the CXCL8 backbone (1.17 A rmsd), but not all sidechains orient as in CXCL8. Most notably, the methyl and sidechain of NAc-Pro^{1} are oriented opposite to the corresponding $E^{29}S^{30}$ atoms.

3.4 Molecular Dynamics (MD)

The MD results for the four isomer combinations of all trans NAc-PGP are presented (Fig. 4). The histograms are the frequency of the C (Acetyl)-N(Pro_1)-C_α(Pro_3)-COO(Pro_3) improper dihedral angle sorted into 20° bins. The red lines are the Gaussian fit of the histogram. The standard deviations for the four isomers were all 55°. The acetyl and carboxylate groups for the LD- and DL- NAc-PGP isomers are populated mostly in the *anti* position. The acetyl and carboxylate groups for the LL- isomer are commonly in the (+)-*gauche* conformation, and the DD- isomer is in the (−)-*gauche* conformation. The most probable conformations are diagrammed (Fig. 4).

3.5 DD-NAc-PGP blocks chemotaxis to LL--NAc-PGP and CXCL8

We tested the four chiral isomers as previously described (Weathington et al., 2006) for their ability to cause both neutrophil (data not shown) and HL-60 cell chemotaxis. The chemotactic index of LL-NAc-PGP including S.E.M. (number of cells per well migrating to LL-NAc-PGP divided by the number of cells migrating to media alone) was 2.37 ± 0.22. Fig. 6 shows that a D-proline on either the N or C terminus of the peptide results in a significant decrease in chemotactic activity when compared to the LL-NAc-PGP. Having a single D-proline in the N terminal position has only a small effect (only 20–25% decrease) on chemotaxis compared to LL-NAc-PGP. Whereas replacing the C terminal proline with a D-proline leads to 50% reduction in chemotaxis compared to LL-NAc-PGP suggesting this area is likely more important in receptor interaction. Interestingly, the DD-isomer is not chemotactic (Fig. 6) but is able to dose dependently inhibit chemotaxis by the LL-isomer and by CXCL8 (Fig. 7).

The specificity of the interaction of DD-NAc-PGP with the CXCR1 and 2 receptors was evaluated by testing it against fMLP and LTB4, two chemokines which do not act via the same receptors as CXCL8 yet cause neutrophil chemotaxis. DD-NAc-PGP showed no effect on chemotaxis to fMLP or LTB4 while chemotaxis to both CXCL8 and NAc-PGP were inhibited by preincubation of cells with DD-NAc-PGP (Fig. 8) The chemotactic indeces of CXCL8, LL-NAc-PGP, fMLP, and LTB4 were 2.72 ± 0.30, 2.37 ± 0.22, 1.64 ± 0.08, and 1.59 ± 0.22, respectively.

3.6 Competition between DD-NAc-PGP andr [125I]-CXCL8 for binding to neutrophils in a radioreceptor assay

To determine whether the inhibitory effect of DD-NAc-PGP on chemotaxis might be at the level of receptor antagonism, we investigated whether DD-NAc-PGP competed with CXCL8 for binding to human neutrophils in a radioreceptor assay. At peptide concentrations similar to those used earlier (Weathington et al., 2006), we found that DD-NAc-PGP could dose-dependently block the specific binding of radiolabeled CXCL8 (Fig. 9). This suggests that the inhibition of chemotaxis is likely due to a direct interaction of DD-NAc-PGP with a binding pocket on CXCR1 and/or CXCR2.

Recently, the ability of NAc-PGP to compete in a CXCL8 radioreceptor assay was questioned due to an inability to repeat our earlier finding (de Kruijf et al., 2010). Since NAc-PGP is at least 1000 fold weaker in binding to CXCR1/2 compared to CXCL8 (Weathington et al., 2006) we suspected that de Kruijf et. al's failure to show competition was due to their adding NAc-PGP simultaneously with radiolabeled CXCL8 to neutrophils rather than preincubating neutrophils with NAc-PGP for 30 min prior to radiolabeled CXCL8 addition. Consistent with this idea, when we add DD-NAc-PGP simultaneously with radiolabeled CXCL8 we also failed to see competition (compare pre-incubation with simultaneous addition, Fig. 9).

4. Discussion

Our earlier work elucidated a role for NAc-PGP in on-going lung inflammation as represented in Fig. 10A. Upon insult to the airway there is a release of CXCL8 (by epithelium and/or resident monocyte/macrophages) resulting in recruitment of neutrophils. The result of this neutrophil influx is a release of the enzymes necessary to breakdown collagen producing the NAc-PGP peptide. This peptide then binds to CXCR1 and/or CXCR2 to continue recruiting neutrophils to the site. Growing knowledge of a role of NAc-PGP in disease suggests a need for therapeutics aimed at inhibiting this pathway (Snelgrove et al., 2010). Here we have studied the D- analogs of NAc-PGP both structurally and biologically as potential antagonists for CXCL8 receptors (Fig. 10B).

The two enantiomeric pairs LL-NAc-PGP and DD-NAc-PGP, and LD-NAc-PGP and DL-NAc-PGP, gave mirror image CD and identical NMR spectra (Figs. 1–3). We have previously reported the solution structure of LL-NAc-PGP as a mixture of the four possible *cis/trans* isomers, all in extended conformations (Lee et al., 2001). We have extended those results to the three other chiral isomers.

The NMR chemical shift is a function of the type of atom and the environment about the atom. With greater structural changes resulting in larger associated chemical shift changes. Because glycine is achiral, we expect the mixed DL- and LD- isomers to have identical NMR spectra, but to possibly differ from the DD- and LL- isomer spectra. Therefore, the NAc-PGP LL- and DD- isomers are expected to have similar ^{1}H and ^{13}C NMR spectra with respect to chemical shifts, coupling patterns, and peak intensities. Our NMR data clearly show the presence of rotational isomers and our spectra are consistent with those reported for other short proline-containing peptides (Stimson et al., 1977). The H^{α} and H^{N} protons as well as the C^{α} and carbonyl carbons are indicators of changes in the backbone conformation or environment, and changes in these chemical shifts or coupling constants would be consistent with differences in backbone structures. The two pairs of diastereomers show different NMR spectra. However, the differences in chemical shifts between L- and D-isomers are smaller than the differences between *cis* and *trans* isomers. This implies that the local environment does not change significantly with chirality. The NOESY spectra of the two sets of diastereomers are different with respect to the intensity of the intra-residue and i, i+1 contacts. However, there are no additional long-range NOESY contacts, which would be expected for helix or turn structures. These NMR data, along with the CD results, are consistent with the hypothesis that in solution the NAc-PGP isomers are families of extended peptides.

When one compares the *cis* and *trans* isomers, there are large shift differences, indicating large local changes between these isomers. For example, there is a 2 ppm change in the Pro-1 C^{γ} between Pro-1 *cis* and *trans*, but there is also a 0.1 ppm change in the Pro-3 C^{γ}. The isomer ratios were determined from ^{13}C NMR data (Table I). The peptide chirality had little effect on the proline *trans/cis* ratio. The *trans* isomer was prominent for both Pro^{1} and Pro^{3}, but not in the same ratio. For all four isomers, Pro-1 always had a higher proportion of *trans* than Pro-3. The average *trans/cis* isomer ratio was about 70:30 for Pro-1 and about 60:40 for Pro-3 (Table II). This increase in the *cis* isomer may be explained by two possible affects: a preceding bulky amino acid, such as tryptophan or valine, or for unblocked C-terminal prolines, by high pH (Grathwohl and Wuthrich, 1976; O'Neal et al., 1996). From work on short peptides, it has been shown that a preceding glycine favors the trans/cis ratio up to 90:10, whereas at high pH the ratio can approach 50:50. Thus for NAc-PGP at pH 5.5, the stabilization of the Pro-3 cis isomer as compared to Pro-1 may be explained as a pH effect. The question of whether the cis and trans isomers both bind and with equal or differing affinities must await further structure activity relationship studies.

When the NMR data are used to calculate structures, it is clear that the backbones of the chiral isomers are extended conformations (Fig. 4). Looking down the peptide backbone (Fig. 4) the differences of the carbonyl and sidechain orientations are clear. When we aligned the backbone atoms of LL-NAc-PGP and DD-NAc-PGP to the $S^{30}G^{31}P^{32}$ of the previously published CXCL8 structure (Fig. 4,5), the backbone atoms of the LL- isomer align almost identically to the CXCL8 backbone with the rmsd of the 11 fitted atoms as 0.45 A. The orientations for all carbonyls and sidechains are also similar to CXCL8. The DD- isomer backbone also matches well with the CXCL8 backbone (1.17 A rmsd), but the sidechains and carbonyls of the C- terminus orient opposite that in CXCL8. The molecular dynamics studies indicate that these conformations follow a Gaussian distribution and are maintained over time. Perhaps there are interactions that are key to receptor function, possibly hydrogen bonds that are formed to the C-terminus carbonyls that are lost in the case of the DD- isomer. Perhaps the acetyl carbonyl group may hydrogen bond at a more distant site and give rise to tighter binding.

In terms of structure function relationships, the results fit well with what is known about CXCL8 (Skelton et al., 1999). Specifically, in this family, chemotactic activity is maintained in spite of considerable variation in the particular amino acid that is N terminal to the “GP” motif and DL-NAc-PGP had the most modest loss of activity, as the GP portion should match exactly to the LL- isomer and the SGP portion of CXCL8. There is a more pronounced loss of activity for LD-NAc-PGP. Finally, the DD- isomer shows no chemotactic activity. The inactivity of DD-NAc-PGP could result either from this analog being a CXCR antagonist or from a lack of interaction with the receptor. The former appears to be the case since DD-NAc-PGP dose dependently (Fig. 7) and specifically (Fig. 8) blocked the chemotactic activity of LL-NAc-PGP and CXCL8 (Fig. 7) suggesting the DD- isomer may block the CXCR1 and/or CXCR2 receptors.

Both an X-ray and NMR structure of CXCL8 are available (Baldwin et al., 1991; Skelton et al., 1999). However there is no structure of either the CXC receptor alone or in complex with CXCL8. Early mutation studies were critical in determining the regions of CXCL8 involved in the interaction with the receptor and these include the characteristic ELR (residues 4–6) motif, a flexible N-loop (residues 10–17) and the $G^{31}P^{32}$ region (Hammond et al., 1996). The N-loop is seen in two conformations in both the X-ray and NMR structures. In the wild type, CXCL8 P^{32} is found in the “proline binding groove” which consists of a hydrophobic pocket defined by the residues of the N-loop and the region around R^{47} of CXCL8. When the NMR structure of a peptide of the CXC receptor bound to CXCL8 was determined, the receptor peptide displaced P^{32} and occupied this proline binding groove. This suggests that once displaced the $G^{31}P^{32}$ region must then interact with the receptor in an as yet uncharacterized manner. Our results suggest that there is a well defined binding pocket for the “GP” motif on the receptor providing molecular interactions that are critical to activation of the receptor.

Consistent with this idea, is the demonstration that DD-NAc-PGP blocks the binding of [125I] labeled CXCR8 in a radioreceptor assay (Fig. 9). Not surprisingly the affinity of NAc-PGP binding to CXCR1 and/or CXCR2 is less than that of CXCL8 as demonstrated by the inability of the peptide to compete for binding unless neutrophils are preincubated with NAc-PGP as compared to being added simultaneously to cells along with CXCL8 (Fig. 9) (de Kruijf et al., 2010). This lesser affinity may result from NAc-PGP contacting a single site on CXCR1/2 while CXCL8 undoubtedly contacts multiple sites on the receptor. Also consistent with a NAc-PGP binding site on CXCR1/2 is our present demonstration of the ability to design a CXCL8 receptor antagonist (i.e. DD-NAc-PGP) based on the structure of the peptide. This small peptide could be easily delivered to the lung via aerosolization and the D- amino acid should provide additional protection against protease degradation. Thus

DD-NAc-PGP would have a longer half-life in the lungs. We conclude that the D- isomers of NAc-PGP, and most importantly the DD-isomer could serve as the lead compound for novel potential therapeutic agents in lung diseases with chronic neutrophil influx.

Acknowledgments

JEB is funded through NIH (HL07783, HL090999 and HL087824).

This project was supported in part by grants from the NHLBI. The content is solely the responsibility of the authors and does not necessarily represent the official views of the NHLBI nor NIH. NAMD was developed by the Theoretical and Computational Biophysics Group in the Beckman Institute for Advanced Science and Technology at the University of Illinois at Urbana-Champaign. The Molecular Dynamics calculations were run using the Ferrum cluster at ferrum.cis.uab.edu.

References

Baldwin ET, Weber IT, St Charles R, Xuan JC, Appella E, Yamada M, Matsushima K, Edwards BF, Clore GM, Gronenborn AM, et al. Crystal structure of interleukin 8: symbiosis of NMR and crystallography. Proc Natl Acad Sci U S A. 1991; 88:502–506. [PubMed: 1988949]

Cerutti DS, Duke RE, Darden TA, Lybrand TP. Staggered Mesh Ewald: An extension of the Smooth Particle-Mesh Ewald method adding great versatility. J Chem Theory Comput. 2009; 5:2322. [PubMed: 20174456]

de Kruijf P, Lim HD, Overbeek SA, Zaman GJ, Kraneveld AD, Folkerts G, Leurs R, Smit MJ. The collagen-breakdown product N-acetyl-Proline-Glycine-Proline (N-alpha-PGP) does not interact directly with human CXCR1 and CXCR2. Eur J Pharmacol. 2010; 643:29–33. [PubMed: 20599927]

Gaggar A, Jackson PL, Noerager BD, O'Reilly PJ, McQuaid DB, Rowe SM, Clancy JP, Blalock JE. A novel proteolytic cascade generates an extracellular matrix-derived chemoattractant in chronic neutrophilic inflammation. J Immunol. 2008; 180:5662–5669. [PubMed: 18390751]

Grathwohl C, Wuthrich K. The X-Pro peptide bond as an nmr probe for conformational studies of flexible linear peptides. Biopolymers. 1976; 15:2025–2041. [PubMed: 963241]

Hammond ME, Shyamala V, Siani MA, Gallegos CA, Feucht PH, Abbott J, Lapointe GR, Moghadam M, Khoja H, Zakel J, Tekamp-Olson P. Receptor recognition and specificity of interleukin-8 is determined by residues that cluster near a surface-accessible hydrophobic pocket. J Biol Chem. 1996; 271:8228–8235. [PubMed: 8626516]

Hardison MT, Galin FS, Calderon CE, Djekic UV, Parker SB, Wille KM, Jackson PL, Oster RA, Young KR, Blalock JE, Gaggar A. The presence of a matrix-derived neutrophil chemoattractant in bronchiolitis obliterans syndrome after lung transplantation. J Immunol. 2009; 182:4423–4431. [PubMed: 19299743]

Hirayama S, Shiraishi T, Shirakusa T, Higuchi T, Miller EJ. Prevention of neutrophil migration ameliorates rat lung allograft rejection. Mol Med. 2006; 12:208–213. [PubMed: 17225868]

Humphrey W, Dalke A, Schulten K. VMD: visual molecular dynamics. J Mol Graph. 1996; 14:33–38. 27–38. [PubMed: 8744570]

Jacob C, Leport M, Szilagyi C, Allen JM, Bertrand C, Lagente V. DMSO-treated HL60 cells: a model of neutrophil-like cells mainly expressing PDE4B subtype. Int Immunopharmacol. 2002; 2:1647–1656. [PubMed: 12469939]

Lee YC, Jackson PL, Jablonsky MJ, Muccio DD, Pfister RR, Haddox JL, Sommers CI, Anantharamaiah GM, Chaddha M. NMR conformational analysis of cis and trans proline isomers in the neutrophil chemoattractant, N-acetyl-proline-glycine-proline. Biopolymers. 2001; 58:548–561. [PubMed: 11246204]

Mackerell AD Jr. Empirical force fields for biological macromolecules: overview and issues. J Comput Chem. 2004; 25:1584–1604. [PubMed: 15264253]

O'Neal KD, Chari MV, McDonald CH, Cook RG, Yu-Lee LY, Morrisett JD, Shearer WT. Multiple cis-trans conformers of the prolactin receptor proline-rich motif (PRM) peptide detected by reverse-phase HPLC, CD and NMR spectroscopy. Biochem J. 1996; 315 (Pt 3):833–844. [PubMed: 8645165]

O'Reilly P, Jackson PL, Noerager B, Parker S, Dransfield M, Gaggar A, Blalock JE. N-alpha-PGP and PGP, potential biomarkers and therapeutic targets for COPD. Respir Res. 2009a; 10:38.

O'Reilly PJ, Hardison MT, Jackson PL, Xu X, Snelgrove RJ, Gaggar A, Galin FS, Blalock JE. Neutrophils contain prolyl endopeptidase and generate the chemotactic peptide, PGP, from collagen. J Neuroimmunol. 2009b; 217:51–54.

Pfister RR, Haddox JL, Sommers CI. Injection of chemoattractants into normal cornea: a model of inflammation after alkali injury. Invest Ophthalmol Vis Sci. 1998; 39:1744–1750. [PubMed: 9699566]

Pfister RR, Haddox JL, Sommers CI, Lam KW. Identification and synthesis of chemotactic tripeptides from alkali-degraded whole cornea. A study of N-acetyl-proline-glycine-proline and N-methyl-proline-glycine-proline. Invest Ophthalmol Vis Sci. 1995; 36:1306–1316. [PubMed: 7775108]

Phillips JC, Braun R, Wang W, Gumbart J, Tajkhorshid E, Villa E, Chipot C, Skeel RD, Kale L, Schulten K. Scalable molecular dynamics with NAMD. J Comput Chem. 2005; 26:1781–1802. [PubMed: 16222654]

Rowe SM, Jackson PL, Liu G, Hardison M, Livraghi A, Solomon GM, McQuaid DB, Noerager BD, Gaggar A, Clancy JP, O'Neal W, Sorscher EJ, Abraham E, Blalock JE. Potential role of high-mobility group box 1 in cystic fibrosis airway disease. Am J Respir Crit Care Med. 2008; 178:822–831. [PubMed: 18658107]

Skelton NJ, Quan C, Reilly D, Lowman H. Structure of a CXC chemokine-receptor fragment in complex with interleukin-8. Structure. 1999; 7:157–168. [PubMed: 10368283]

Snelgrove RJ, Jackson PL, Hardison MT, Noerager BD, Kinloch A, Gaggar A, Shastry S, Rowe SM, Shim YM, Hussell T, Blalock JE. A critical role for LTA4H in limiting chronic pulmonary neutrophilic inflammation. Science. 2010; 330:90–94. [PubMed: 20813919]

Stimson ER, Zimmerman SS, Scheraga HA. Conformational studies of oligopeptides containing proline and glycine. Macromolecules. 1977; 10:1049–1060. [PubMed: 916731]

Weathington NM, van Houwelingen AH, Noerager BD, Jackson PL, Kraneveld AD, Galin FS, Folkerts G, Nijkamp FP, Blalock JE. A novel peptide CXCR ligand derived from extracellular matrix degradation during airway inflammation. Nat Med. 2006; 12:317–323. [PubMed: 16474398]

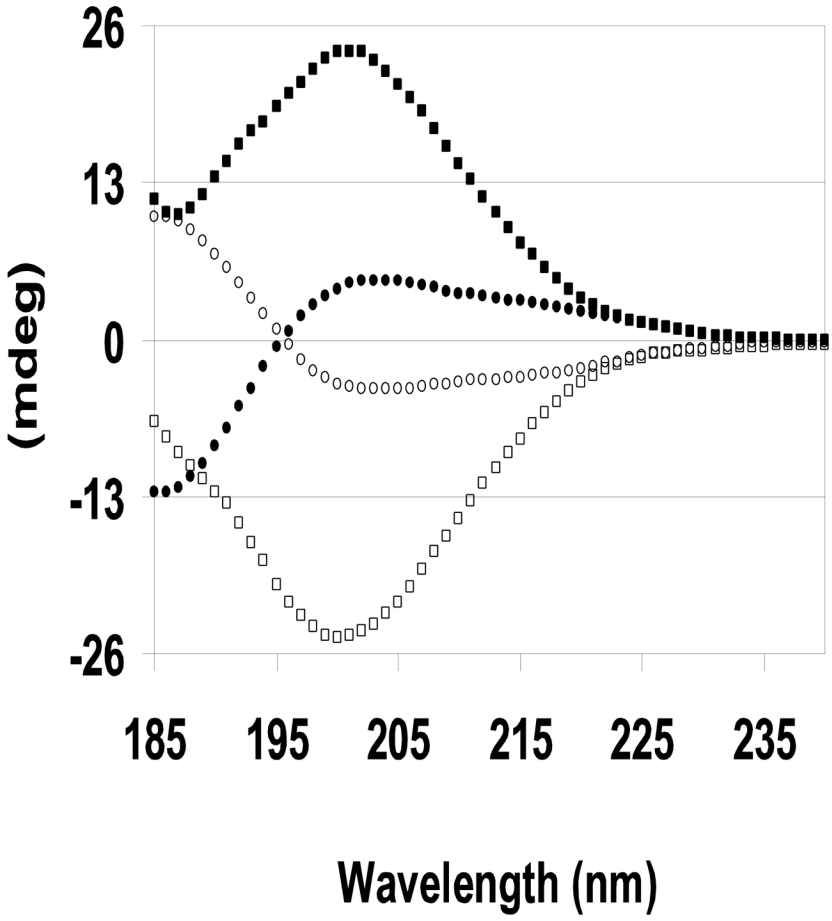

FIG. 1. Far UV CD spectra of the four D- and L- NAc-PGP isomers

2.0 mg/ml, pH 5.5, 0.1 mm cell, and 20°C. □ LL-NAc-PGP, ■ DD-NAc-PGP, ● LD-NAc-PGP, ○ DL-NAc-PGP.

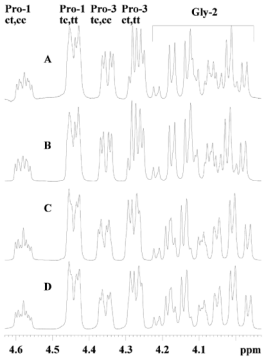

FIG. 2. ^{1}H NMR spectra of the H$^{\alpha}$ region of the four D- and L- NAc-PGP isomers

A, LL-NAc-PGP; *B*, DD-NAc-PGP; *C*, DL-NAc-PGP; *D*, LD-NAc-PGP. The cis and trans proline peaks are labeled as *cis*-Pro^{1} *cis*-Pro^{3}, cc; *trans*-Pro^{1} *trans*-Pro^{3} tt; etc. Not all glycine peaks are shown.

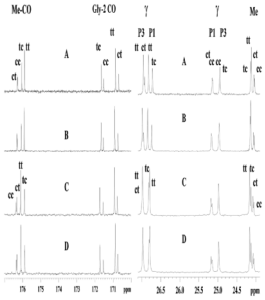

FIG. 3. ^{13}C NMR spectra of the glycine and Me carbonyl, and C$^{\gamma}$ regions of the four D- and L-NAc-Pro-Gly-Pro isomers

A, LL-NAc-PGP; *B*, DD-NAc-PGP; *C*, DL-NAc-PGP; *D*, LD-NAc-PGP.

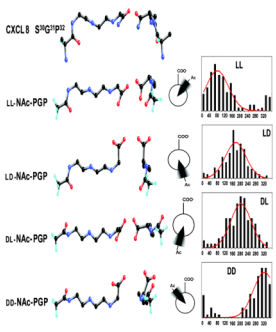

FIG. 4. Models of NAc-Pro-Gly-Pro and CXCL8

Ball and stick model of the putative binding domain of CXCL8 ($S^{31}G^{32}P^{33}$). Aligned beneath are the ball and stick models of the isomers of NAc-PGP matched by heavy atoms. Middle structures are rotated 90° so as to look down the peptide backbone. The Newman projections are of the acetyl and carboxylate along the improper dihedral angle on the most probable conformation. The histograms from the molecular dynamics show frequency vs. angle of the C(Acetyl)-N(Pro_1)-C_α(Pro_3)-COO(Pro_3) improper dihedral angle. The angles are group between 0° and 360° in 20° bins. The solid lines are the Gaussian distributions.

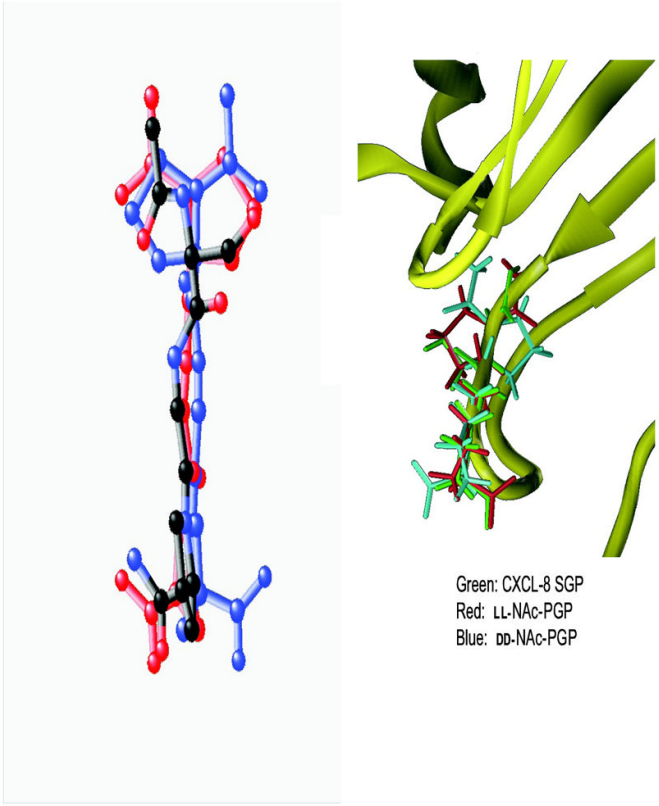

FIG. 5. Superposition of CXCL8 (1ilq) and NAc-PGP

LL-NAc-PGP is red and DD-NAc-PGP) is blue. The NAc-PGP molecules are matched to the CXCL8 backbone. A) CXCL8 with atoms colored by atoms type (black carbon, red oxygen, blue nitrogen) B) CXCL8 is shown as a ribbon with $S^{30}G^{31}P^{32}$ in green.

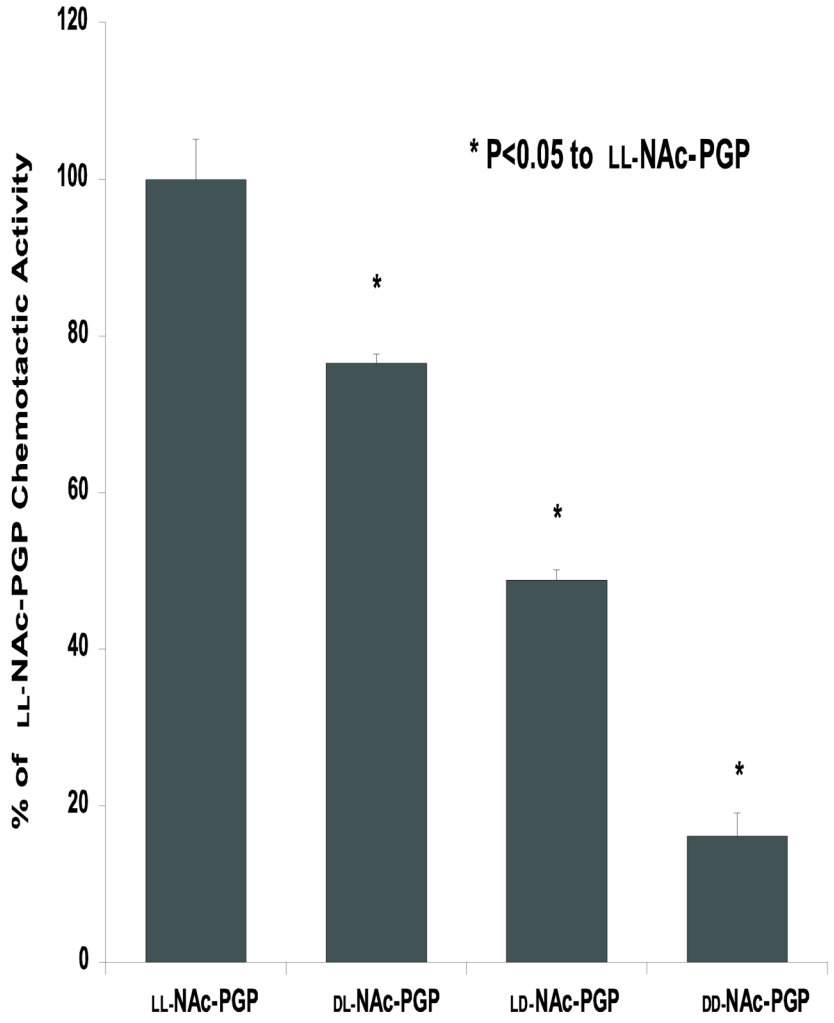

FIG. 6. Chemotactic activity of D- isomers of NAc-PGP

Standard chemotaxis assays were performed with the indicated isomer of Nac-PGP at 3 μM. Data are expressed as a percentage of the chemotactic activity of the LL-Nac-PGP, which had a chemotactic index of 2.75 ± 0.28. Data represents the mean % activity ± S.E.M. of 6 replicates. Isomers differ from one another at P value <0.01 by ANOVA. The chemotaxis seen with DD-Nac-PGP is residual cellular migration.

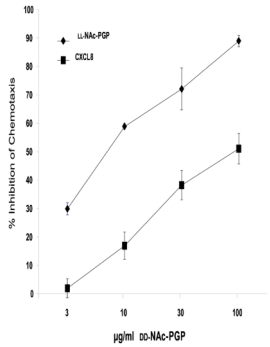

FIG. 7. DD-NAc-PGP inhibits chemotaxis to LL-NAc-PGP and CXCL8

Cells were incubated with 100, 30, 10, 3 µg/ml DD-NAc-PGP, or CXCL8 (0.7 nM) or NAc-PGP (0.032 mM) for 30 min at room temperature. CXCL8 or NAc-PGP was added to the lower wells of chemotaxis chambers, and DD-NAc-PGP-treated cells were added to the upper wells and incubated for 1.5h at 37°C. The chemotactic indeces for CXCL8 or NAc-PGP alone were 2.72 ± 0.30 and 2.37 ± 0.22, respectively. Data represent the % inhibition ± S.E.M. compared to the control of CXCL8 or NAc-PGP alone.

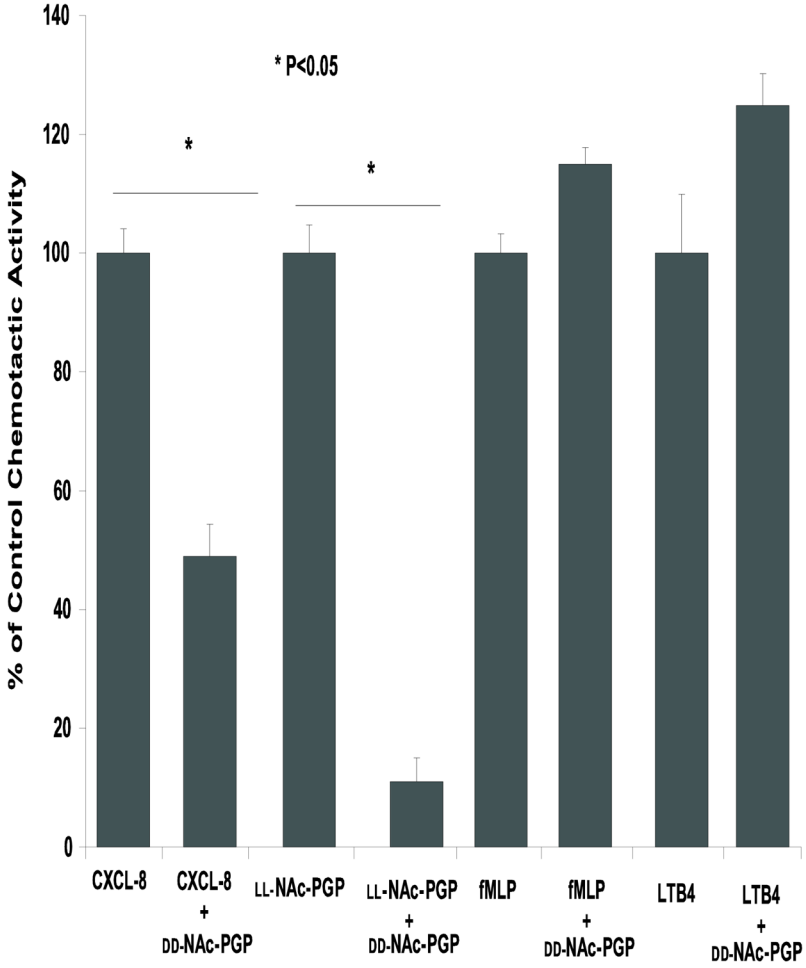

FIG. 8. DD-NAc-PGP inhibits chemotaxis to CXCL8 but not to control chemoattractants

Cells were incubated with 0.032 mM DD-NAc-PGP or media for 30 min at room temperature. CXCL8 (0.7 nM), LL-NAc-PGP (0.032 mM), fMLP(30 nM), or LTB4(30nM) was added to the lower wells of chemotaxis chambers, and DD-NAc-PGP-treated or control cells were added to the upper wells and incubated for 1.5h at 37°C.

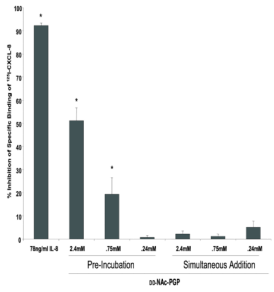

FIG. 9. DD-NAc-PGP inhibits [125I]-CXCL8 binding

Indicated concentrations of DD-NAc-PGP were either pre-incubated at 4°C for 30 min prior to radioligand addition, or added simultaneously with 7.8ng/ml [125I]-CXCL8. Cells were then kept at 4°C for 90 min to allow binding to occur and resulting cell associated radiation was measured using a Packerd Gamma Counter. (* P value<0.05)

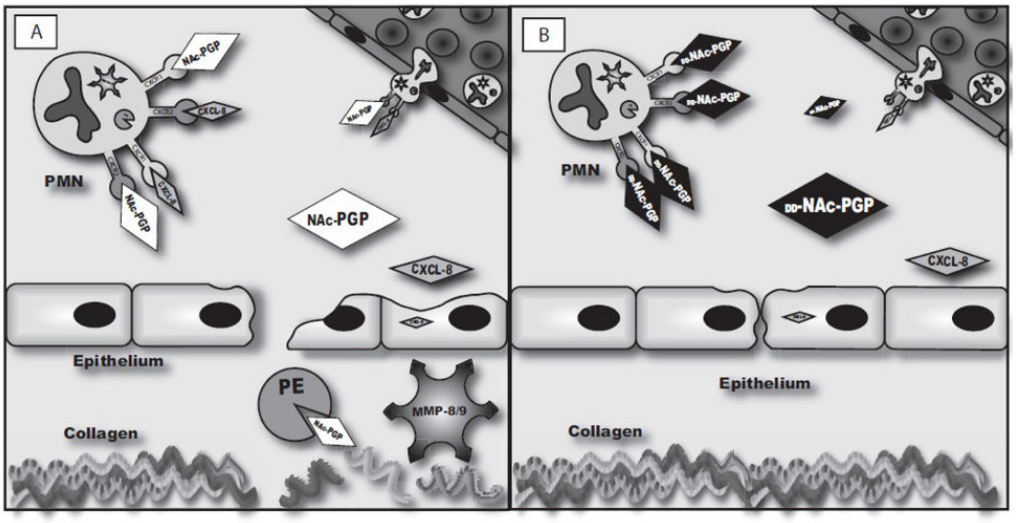

FIG. 10. Potential Effects of the isomers of NAc-PGP on neutrophilic inflammation

Fig. 10A

Upon injury or insult the airway epithelium releases CXCL8. CXCL8 draws neutrophils in from the periphery at which point they either actively release MMP8 and/or 9 and PE or release it upon apoptosis. The MMPs perform an initial cleavage of collagen creating an optimum substrate for the final catalysis by PE to release PGP. PGP, acting via the same CXCR1 and CXCR2 receptors that CXCL8 utilizes, can cause further neutrophil influx and activation.

Fig. 10B

DD-NAc-PGP binds at CXCR1 and 2 on neutrophils but prevents the activation. This blocks the downstream release of proteases resulting in less collagen cleavage and epithelial damage, ultimately blocking the chronic neutrophil influx.

Table I

NAc-PGP cis/trans isomer ratios for each chiral molecule

Chiral Isomer	trans-trans	trans-cis	cis-trans	cis-cis
LL-NAc-PGP	41[a]	28	17	14
DD-NAc-PGP	42	28	17	13
DL-NAc-PGP	44	26	17	12
LD-NAc-PGP	44	26	17	12

[a]Ratios are the average of the ^{13}C of Gly-C^{α}, Me-CO, and Me ratios.

Table II

NAc-PGP cis/trans isomer ratios, average values

Conformational Isomer	%Trans	% Cis
Pro-3 trans	72[a]	28
Pro-3 cis	69	31
Pro-1 trans	61	39
Pro-1 cis	57	43

[a] Values are derived from Table I and are an average of all four DL-isomers